Supplementary Information

Functionalized resorcin[4]arene-based coordination polymers as heterogeneous catalyst for click reactions

Fei-Fei Wang,[a†] Jia-Hui Li,[a†] Hai-Yan Liu,[b] Shu-Ping Deng,[b] Ying-Ying Liu*[a] and Jian-Fang Ma*[a]

[a]*Key Lab of Polyoxometalate Science, Department of Chemistry, Northeast Normal University, Changchun 130024, China*

[b]*Key Lab of Chemical Additive Synthesis and Separation, Department of Chemical and Environmental Engineering*, *Yingkou Institute of Technology, Yingkou 115014, China*

Table of Contents

Materials and Instrumentation

Chemicals are purchased commercially. Resorcin[4]arenes ligand was synthesized by the literature procedure.[1] PXRD patterns were measured on a Rigaku Dmax 2000 X-ray diffractometer with graphite-monochromatized Cu Kα radiation. IR spectra were measured on a Mattson Alpha-Centauri spectrometer. Thermogravimetric analysis was performed on a PerkinElmer model TG-7 analyzer. ICP measurements were conducted on a Leeman Laboratories Prodigy inductively coupled plasma-optical atomic emission spectrometer (ICP-AES). C, H, N and S contents were carried out on a Euro vector EA3000 elemental analyzer. The conversions of catalytic substrates were record by GC equipment with FID detector (GC-2014C, Shimadzu, Japan) and capillary (30 m × 0.25 mm i.d., WondaCap 17). ^{1}H NMR data were recorded in $CDCl_3$ on a Bruker 500 MHz.

X-ray crystallography

Single crystal X-ray diffraction data of **1-3** were measured on an Oxford Diffraction Gemini R CCD diffractometer with graphite monochromated Mo Kα radiation (λ = 0.71073 Å) at room temperature. Their crystal structures were solved by direct methods and refined on F^2 by full-matrix least-squares with SHELXL-2018/3.[2-4] Non-hydrogen atoms were located from difference Fourier maps and refined anisotropically. The SQUEEZE function in PLATON was applied for **1-3** during the refinement because of the highly disordered solvents. Their fomula were affirmed by thermogravimentric analysis, electron cloud density and elemental analysis. Crystallographic data are listed in Table S1. Selected bond distances and angles were given in Tables S2-S4.

Experimental Section

Spectroscopic data of L

In the IR spectrum of L, the bands at 1671 cm^{-1}, 1580 cm^{-1}, 1462 cm^{-1}, 1413 cm^{-1} and 791 cm^{-1} are due to the aromatic C=N, C=C and C-H bonds. The bands at 2963 cm^{-1} and 1380 cm^{-1} are owing to -CH_3 groups. The band at 973 cm^{-1} is because of C-O-C bonds and the band at 714 cm^{-1} is assigned to the C-S bonds for 4-MPy.

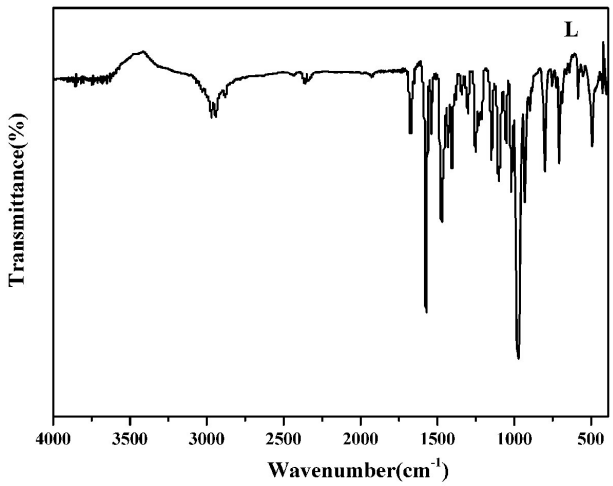

Fig. S1 IR spectrum of L

In the UV-Vis diffuse reflectance spectrum of L, the ligand L exhibits a relatively wide absorption band between 200-310nm, which can be attributed to the π*→n or π*→π transition (Fig. S2).

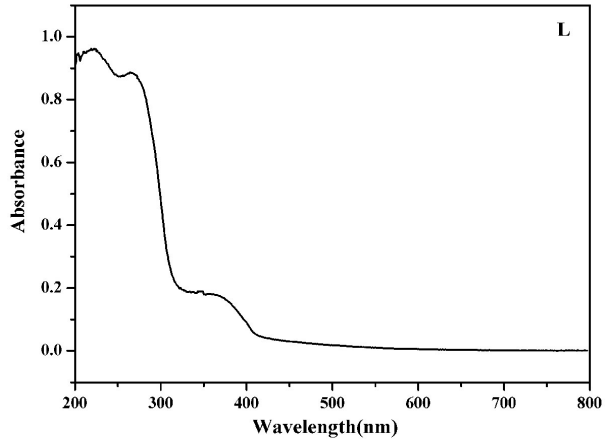

Fig. S2 UV-Vis diffuse reflectance spectrum of L

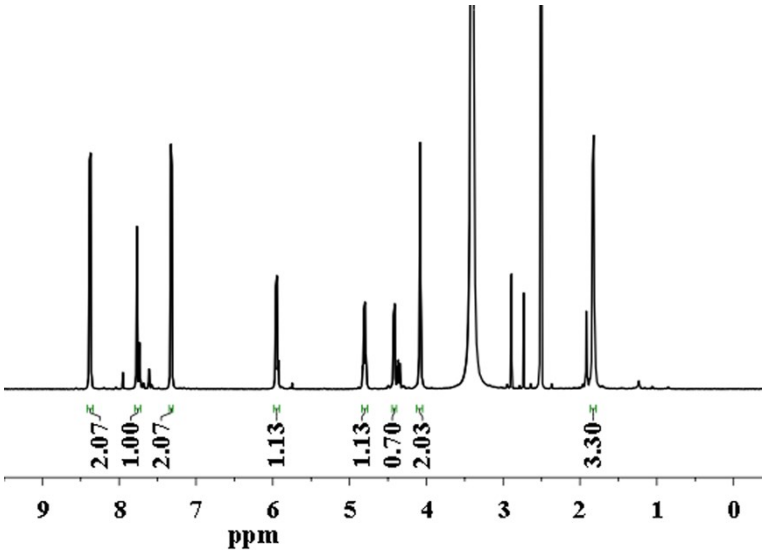

Fig. S3 ^{1}H NMR (500 MHz, DMSO) for L

Procedure for reactions of benzyl azide and phenylacetylene

A mixture of amyl acetate (0.92 mmol) as the internal standard, benzyl azide (1 mmol), alkyne (2 mmol), MeOH (4 mL) and catalyst (5 mg) was put in a 38 mL pressure-proof pipe and stirred at 80°C for 5 h. GC and ^{1}H NMR were used to determine and confirm the conversions (Figs. S7-S18).

Procedure for reactions of β-OH azide and phenylacetylene

The β-OH azide was synthesized in advance from epoxy compound and sodium azide. A mixture of internal standard ethylbenzene (1 mmol), β-OH azide (2 mmol), alkyne (1 mmol), MeOH (4 mL) and catalyst (10 mg) was put in a 38 mL pressure-proof pipe and stirred at 80°C for 8 h. GC and ^{1}H NMR were applied to measure and certify the conversions (Figs. S19-S27). The β-OH azide was synthesized in advance with epoxy and sodium azide according to the literature.

References

[1] L. Wang, T.-T. Guo, J.-C. Ma, Y.-Y. Liu, G.-H. Xu, J.-F. Ma, *ChemistrySelect* 2019, **4**, 7351–7357.

[2] G. M. Sheldrick, *SHELXS-2018, Programs for X-ray Crystal Structure Solution*, University of Göttingen: Göttingen, Germany, 2018.

[3] L. J. Farrugia, *WINGX: A Windows Program for Crystal Structure Analysis*, University of Glasgow: Glasgow, UK, 1988.

[4] G. M. Sheldrick, *SHELXTL-2018, Programs for X-ray Crystal Structure Refinement*, University of Göttingen: Göttingen, Germany, 2018.

Table S1 Crystallographic data and structure refinements for **1-3**

Compound	**1**	**2**	**3**
Formula	$Cu_2C_{122.5}H_{109}N_{10}O_{18}S_8$	$CdC_{82}H_{97}Cl_2N_9O_8S_4$	$Cd_2C_{103}H_{115}N_{10}O_{28}S_4$
Mr	2392.75	1732.4	2053.78
Temperature (K)	293(2)	293(2)	298(2)
Crystal system	Monoclinic	Monoclinic	Orthorhombic
Space group	*I*2/*a*	*P*21/*m*	*Pca*21
a (Å)	21.8025(10)	11.1814(2)	28.6962(18)
b (Å)	22.0950(10)	23.0432(4)	16.3215(10)
c (Å)	48.236(2)	16.9568(4)	20.5240(11)
α(°)	90	90	90
β(°)	90.174(4)	107.771(2)	90
γ(°)	90	90	90
V(Å^3)	23236.4(19)	4160.54(15)	9612.7(10)
Z	8	2	4
D_{calc} (g·cm^{-3})	1.368	1.503	1.585
F(000)	9952	1948	4220
R_{int}	0.0809	0.0418	0.0402
GOF on F^2	0.933	0.969	0.994
$^aR_1$	0.0782	0.0388	0.0527
$^bwR_2$	0.2484	0.1050	0.1467

$^aR_1 = \sum||F_o| - |F_c||/\sum|F_o|$, $^bwR_2 = \{\sum w[(F_o)^2 - (F_c)^2]^2/\sum w[(F_o)^2]^2\}^{1/2}$

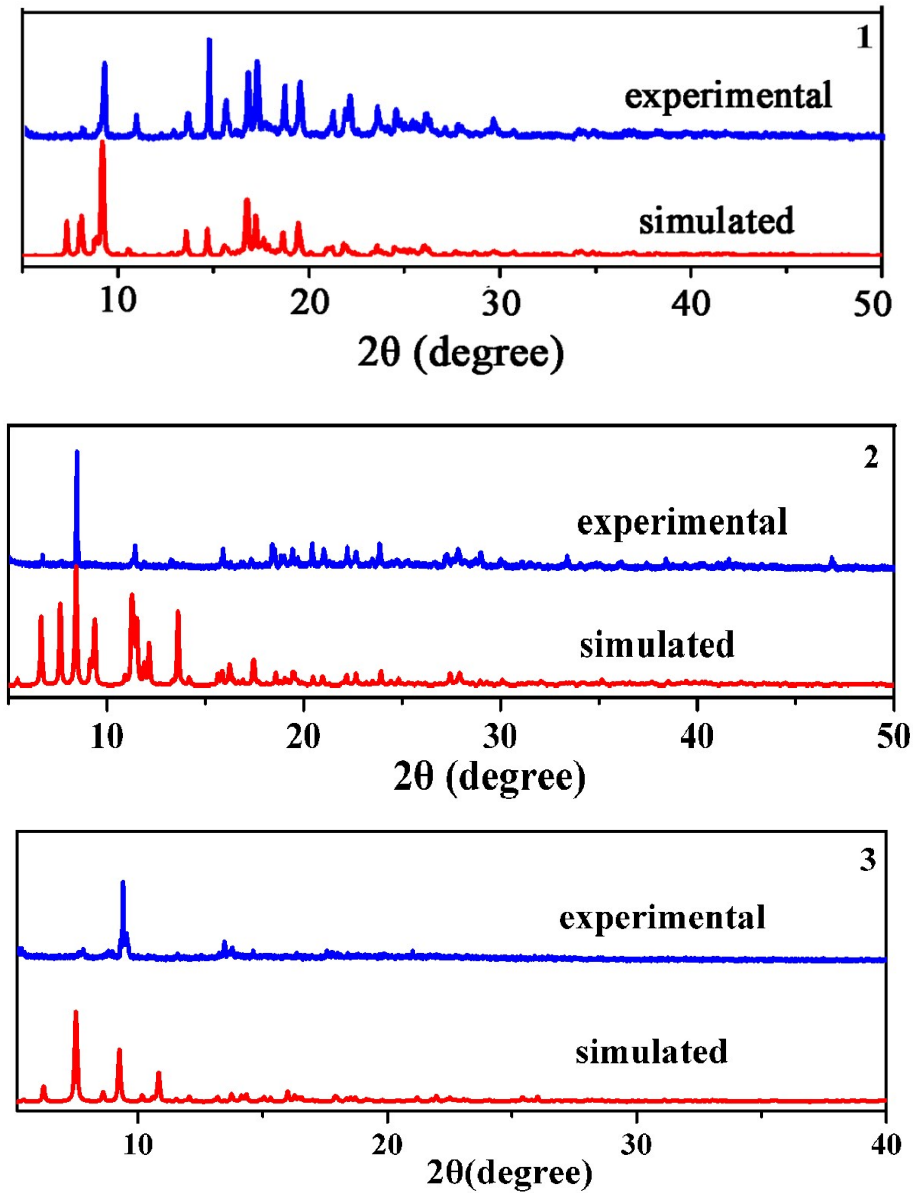

Fig. S4 PXRD curves of **1**-3 simulated (red), experimental (blue).

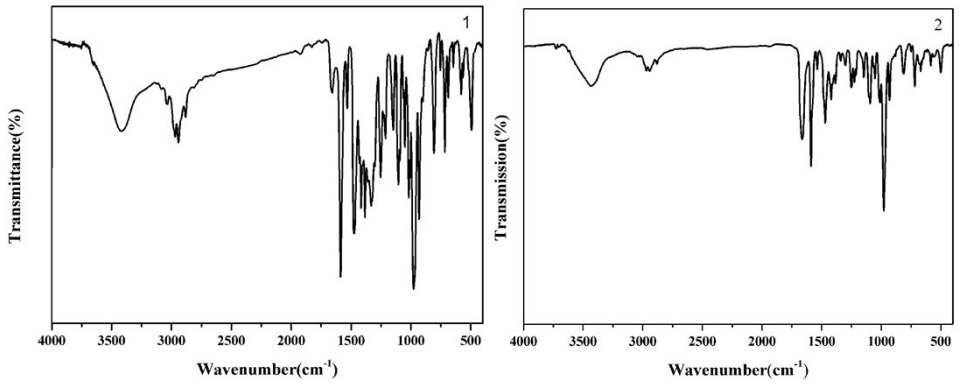

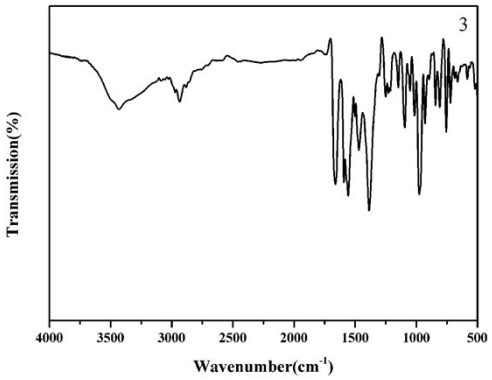

Fig. S5 IR spectra of **1-3**.

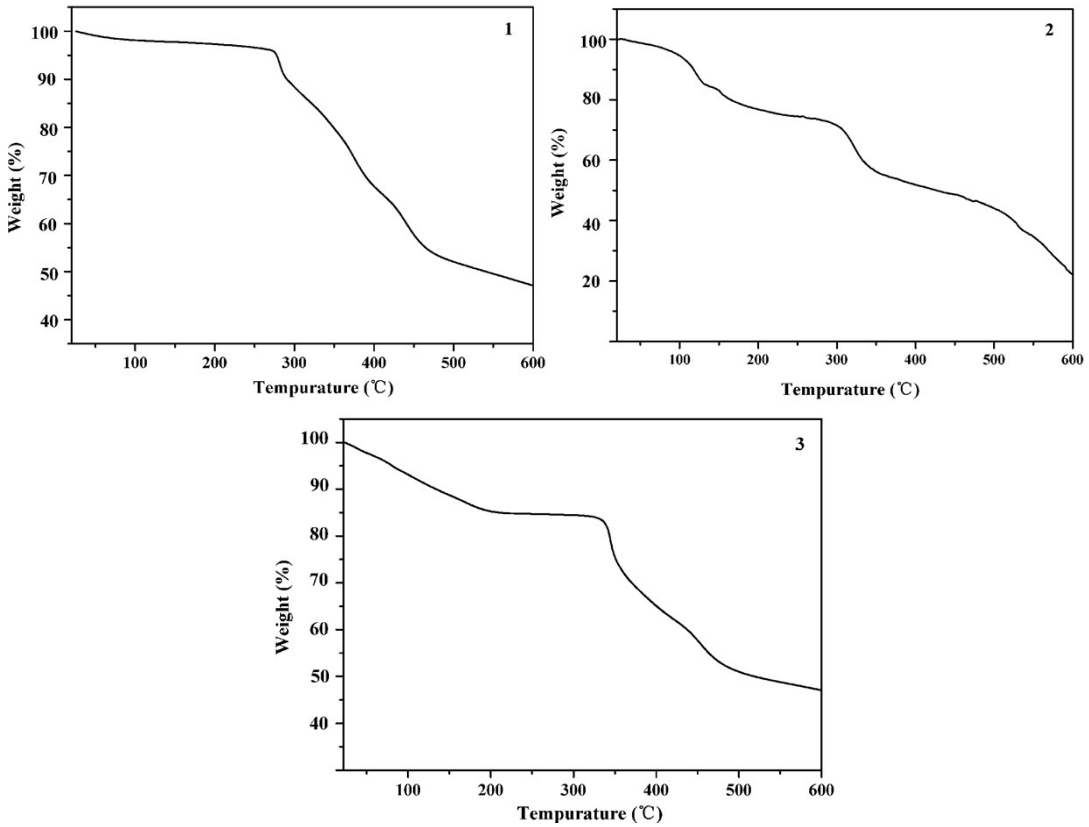

Fig. S6 Thermogravimetric curves of **1-3.**

Table S2. Selected bond distances (Å) and angles (deg) for **1**.

Cu(1)-N(8)	1.991(5)	Cu(1)-N(5)$^{\#1}$	2.034(4)
Cu(1)-N(6)	2.047(5)	Cu(1)-N(7)$^{\#2}$	2.103(5)
Cu(2)-N(4)$^{\#3}$	2.027(5)	Cu(2)-N(1)	2.059(4)
Cu(2)-N(3)	2.059(5)	Cu(2)-N(2)	2.074(5)
N(8)-Cu(1)-N(5)$^{\#1}$	125.0(2)	N(8)-Cu(1)-N(6)	118.2(2)

N(5)$^{\#1}$-Cu(1)-N(6)	100.2(2)	N(8)-Cu(1)-N(7)$^{\#2}$	94.0(2)
N(5)$^{\#1}$-Cu(1)-N(7)$^{\#2}$	109.7(2)	N(6)-Cu(1)-N(7)$^{\#2}$	109.0(2)
N(1)-Cu(2)-N(3)	107.4(2)	N(4)$^{\#3}$-Cu(2)-N(2)	108.97(19)
N(1)-Cu(2)-N(2)	105.02(18)	N(3)-Cu(2)-N(2)	110.2(2)

Symmetry transformations used to generate equivalent atoms: $^{\#1}$ -x+1, -y+2, -z+1; $^{\#2}$ x, -y+3/2, z+1/2; $^{\#3}$ -x+1, y-1/2, -z+1/2.

Table S3. Selected bond distances (Å) and angles (deg) for 2.

Cd(1)-N(1)	2.386(2)	Cd(1)-N(1)$^{\#1}$	2.386(2)
Cd(1)-N(2)$^{\#2}$	2.4377(18)	Cd(1)-N(2)$^{\#3}$	2.4377(18)
Cd(1)-Cl(1)$^{\#1}$	2.5666(6)	Cd(1)-Cl(1)	2.5666(6)
N(1)-Cd(1)-N(1)$^{\#1}$	180.0	N(1)-Cd(1)-N(2)$^{\#2}$	88.01(9)
N(1)$^{\#1}$-Cd(1)-N(2)$^{\#2}$	91.99(9)	N(1)-Cd(1)-N(2)$^{\#3}$	91.99(9)
N(1)$^{\#1}$-Cd(1)-N(2)$^{\#3}$	88.01(9)	N(2)$^{\#2}$-Cd(1)-N(2)$^{\#3}$	180.00(9)
N(1)-Cd(1)-Cl(1)$^{\#1}$	91.15(6)	N(1)$^{\#1}$-Cd(1)-Cl(1)$^{\#1}$	88.86(6)
N(2)$^{\#2}$-Cd(1)-Cl(1)$^{\#1}$	90.65(5)	N(2)$^{\#3}$-Cd(1)-Cl(1)$^{\#1}$	89.35(5)
N(1)-Cd(1)-Cl(1)	88.86(6)	N(1)$^{\#1}$-Cd(1)-Cl(1)	91.14(6)
N(2)$^{\#2}$-Cd(1)-Cl(1)	89.35(5)	N(2)$^{\#3}$-Cd(1)-Cl(1)	90.65(5)
Cl(1)$^{\#1}$-Cd(1)-Cl(1)	180.0		

Symmetry transformations used to generate equivalent atoms: $^{\#1}$-x+2, -y+1, -z; $^{\#2}$ x, y, z-1; $^{\#3}$ -x+2, -y+1, -z+1.

Table S4. Selected bond distances (Å) and angles (deg) for **3**.

Cd(1)-O(12)	2.304(5)	Cd(1)-N(1)	2.327(6)
Cd(1)-N(3)$^{\#1}$	2.320(5)	Cd(1)-O(10)	2.333(6)
Cd(1)-O(14)$^{\#2}$	2.370(7)	Cd(1)-O(13)$^{\#2}$	2.430(5)
Cd(1)-O(11)	2.596(7)	Cd(2)-O(15)	2.450(8)
Cd(2)-O(9)	2.286(7)	Cd(2)-O(11)	2.288(7)
Cd(2)-N(4)$^{\#3}$	2.322(7)	Cd(2)-O(17)$^{\#4}$	2.331(7)
Cd(2)-O(16)$^{\#4}$	2.377(7)	O(16)$^{\#4}$-Cd(2)-O(10)	168.67(18)
Cd(2)-O(10)	2.593(6)	O(15)-Cd(2)-O(10)	95.9(2)
O(12)-Cd(1)-N(3)$^{\#1}$	96.3(2)	O(12)-Cd(1)-N(1)	83.8(2)

N(3)$^{\#1}$-Cd(1)-N(1)	176.7(2)	O(12)-Cd(1)-O(10)	125.2(2)
N(3)$^{\#1}$-Cd(1)-O(10)	88.6(2)	N(1)-Cd(1)-O(10)	88.6(2)
O(12)-Cd(1)-O(14)$^{\#2}$	136.2(2)	N(3)$^{\#1}$-Cd(1)-O(14)$^{\#2}$	91.0(2)
N(1)-Cd(1)-O(14)$^{\#2}$	91.2(2)	O(10)-Cd(1)-O(14)$^{\#2}$	98.0(2)
O(12)-Cd(1)-O(13)$^{\#2}$	82.0(2)	N(3)$^{\#1}$-Cd(1)-O(13)$^{\#2}$	94.5(2)
N(1)-Cd(1)-O(13)$^{\#2}$	88.7(2)	O(10)-Cd(1)-O(13)$^{\#2}$	152.2(2)
O(14)$^{\#2}$-Cd(1)-O(13)$^{\#2}$	54.42(18)	O(12)-Cd(1)-O(11)	51.96(19)
N(3)$^{\#1}$-Cd(1)-O(11)	91.5(2)	N(1)-Cd(1)-O(11)	86.0(2)
O(10)-Cd(1)-O(11)	73.4(2)	O(14)$^{\#2}$-Cd(1)-O(11)	170.99(19)
O(13)$^{\#2}$-Cd(1)-O(11)	133.92(19)	O(9)-Cd(2)-O(11)	125.8(2)
O(9)-Cd(2)-N(4)$^{\#3}$	92.5(3)	O(11)-Cd(2)-N(4)$^{\#3}$	88.0(2)
O(9)-Cd(2)-O(17)$^{\#4}$	85.3(2)	O(11)-Cd(2)-O(17)$^{\#4}$	148.5(2)
N(4)$^{\#3}$-Cd(2)-O(17)$^{\#4}$	96.5(3)	O(9)-Cd(2)-O(16)$^{\#4}$	139.7(2)
O(11)-Cd(2)-O(16)$^{\#4}$	94.5(2)	N(4)$^{\#3}$-Cd(2)-O(16)$^{\#4}$	90.5(3)
O(17)$^{\#4}$-Cd(2)-O(16)$^{\#4}$	54.5(2)	O(9)-Cd(2)-O(15)	100.2(3)
O(11)-Cd(2)-O(15)	81.2(2)	N(4)$^{\#3}$-Cd(2)-O(15)	166.6(3)
O(17)$^{\#4}$-Cd(2)-O(15)	88.7(3)	O(16)$^{\#4}$-Cd(2)-O(15)	82.5(3)
O(9)-Cd(2)-O(10)	51.7(2)	O(11)-Cd(2)-O(10)	74.2(2)
N(4)$^{\#3}$-Cd(2)-O(10)	88.7(2)	O(17)$^{\#4}$-Cd(2)-O(10)	136.9(2)

Symmetry transformations used to generate equivalent atoms: $^{\#1}$ x-1/2, -y-1, z; $^{\#2}$ -x+1/2, y, z-1/2; $^{\#3}$ -x+1/2, y, z+1/2; $^{\#4}$ -x, -y-1, z+1/2.

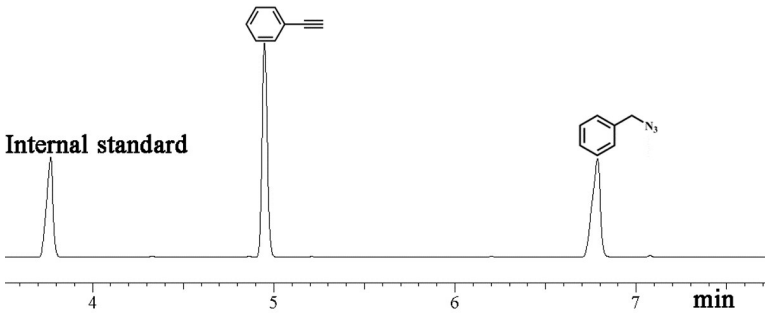

(a)

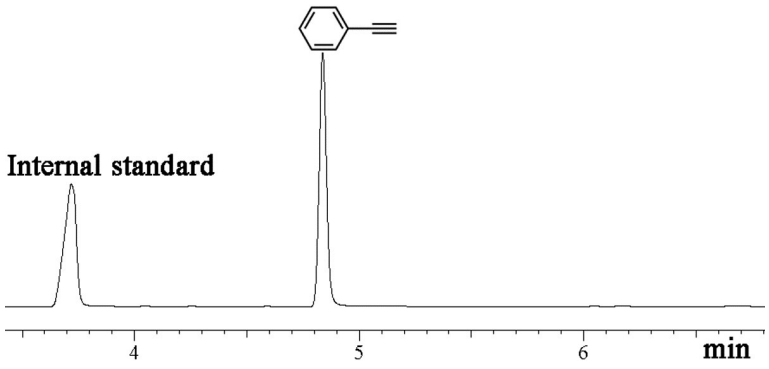
Internal standard
4
5
6
min

(b)

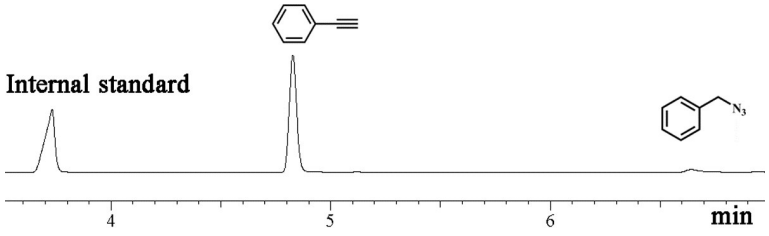
Internal standard
N_3
4
5
6
min

(c)

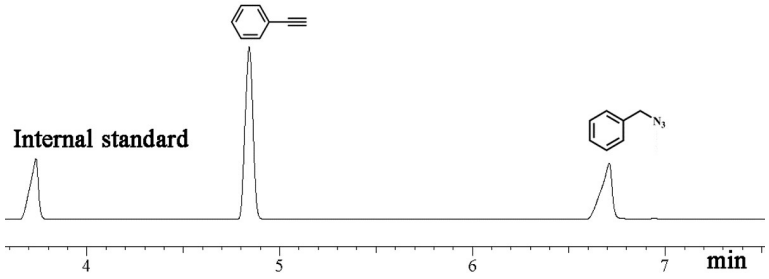
Internal standard
N_3
4
5
6
7
min

(d)

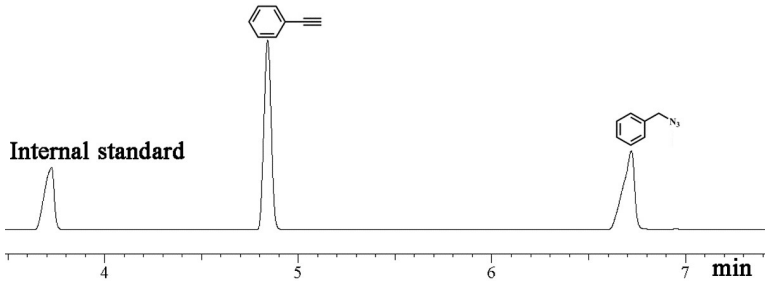
Internal standard
N_3
4
5
6
7
min

(e)

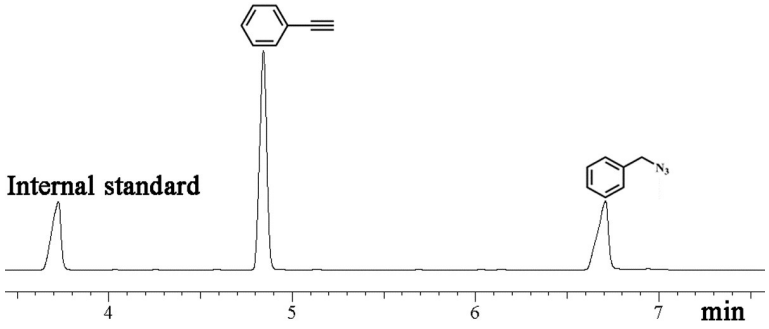
Internal standard
N_3
4
5
6
7
min

(f)

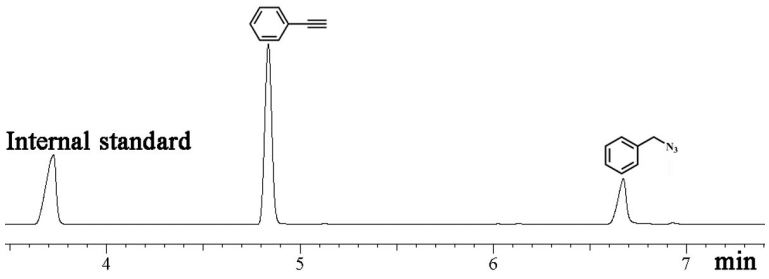

(g)

Fig. S7 GC of reactions of benzyl azide and phenylacetylene under different conditions: (a) **1** (0 mg), MeOH, 5 h, 80°C. (b) **1** (5 mg), MeOH, 5 h, 80°C. (c) **1** (5 mg), EtOH, 5 h, 80°C. (d) **1** (5 mg), MeCN, 5 h, 80°C. (e) **1** (5 mg), MeOH, 5 h, 25°C. (f) **1** (5 mg), MeOH, 5 h, 40°C. (g) **1** (5 mg), MeOH, 5 h, 60 °C.

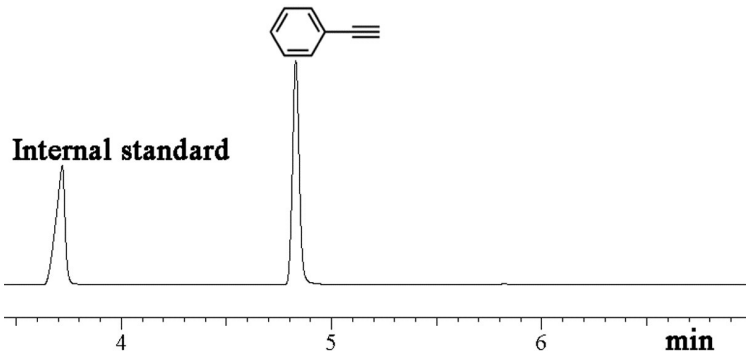

(a)

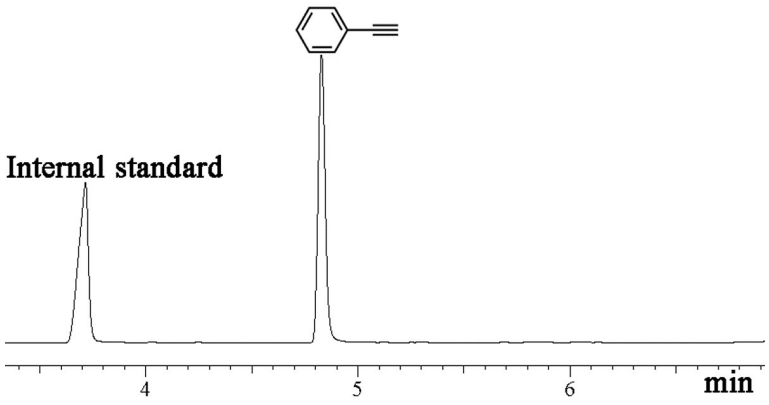

(b)

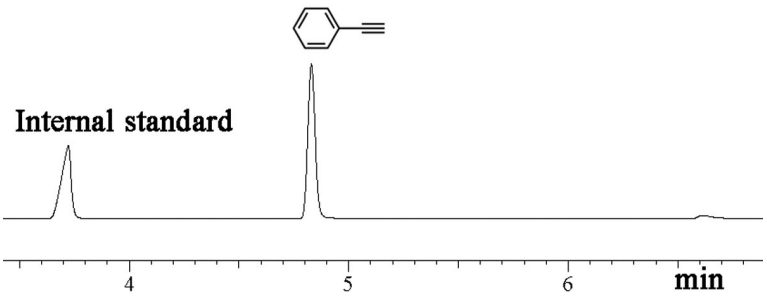
Internal standard
4
5
6
min

(c)

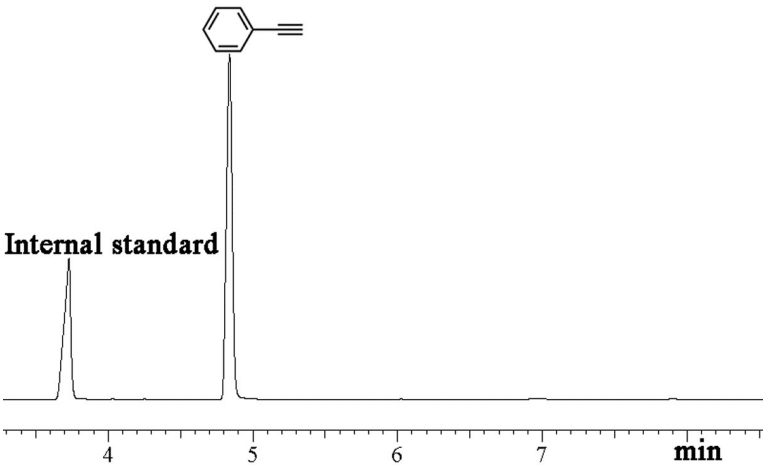
Internal standard
4
5
6
7
min

(d)

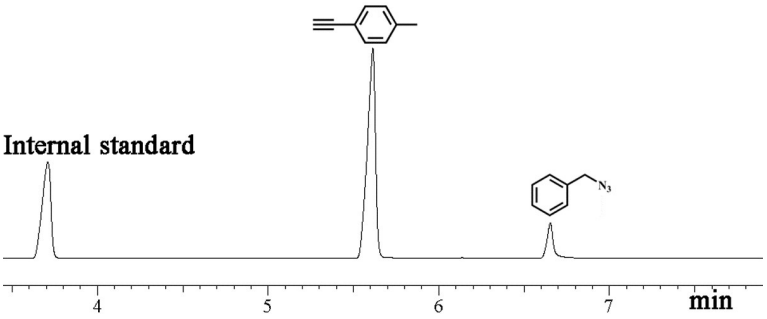
Internal standard
4
5
6
7
min

(e)

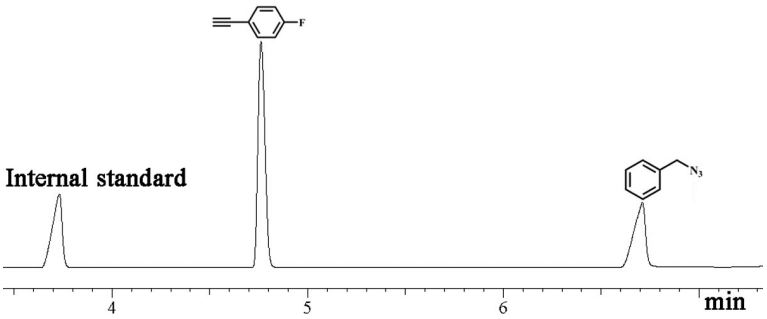
Internal standard
4
5
6
min

(f)

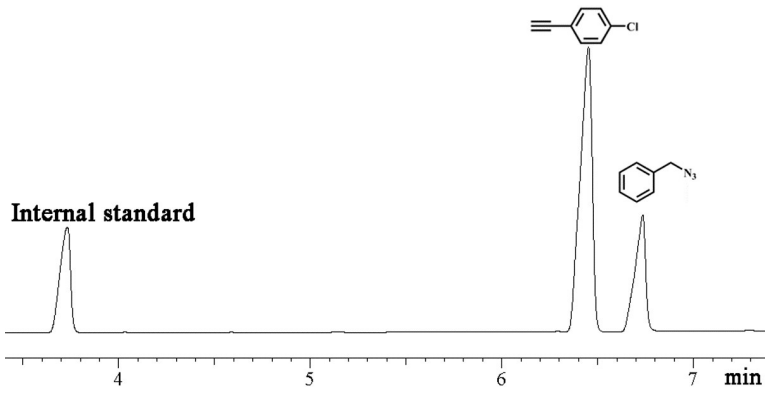

(g)

Fig. S8 GC of reactions of substituted benzyl azides and phenylacetylenes with different groups under the same condition (1 (5 mg), MeOH, 5 h, 80 °C):

(a) 1-(azidomethyl)-4-methyl-benzene and phenylacetylene as substrates.

(b) 1-(azidomethyl)-3-methylbenzene and phenylacetylene as substrates.

(c) 1-(azidomethyl)-2-fluorobenzene and phenylacetylene as substrates.

(d) 1-(azidomethyl)-4-nitrobenzene and phenylacetylene as substrates.

(e) 1-(azidomethyl)benzene and 1-ethynyl-4-methylbenzene as substrates.

(e) 1-(azidomethyl)benzene and 1-ethynyl-4-fluorobenzene as substrates.

(g) 1-(azidomethyl)benzene and 1-ethynyl-4-chlorobenzene as substrates.

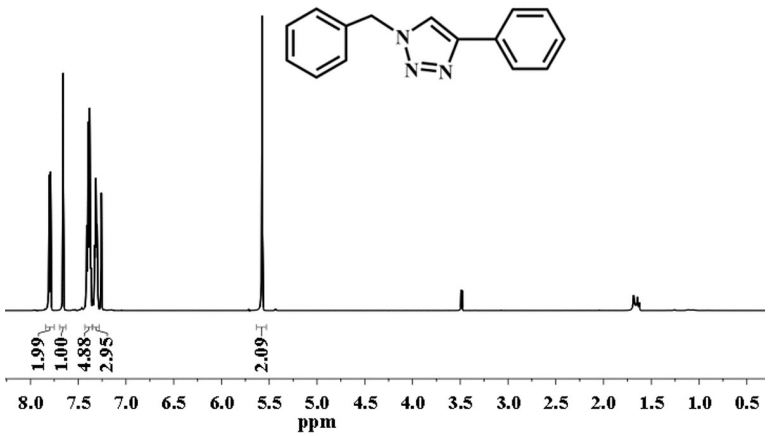

Fig. S9 ^{1}H NMR (500 MHz, $CDCl_3$) for 1-benzyl-4-phenyl-1H-1,2,3-triazole.

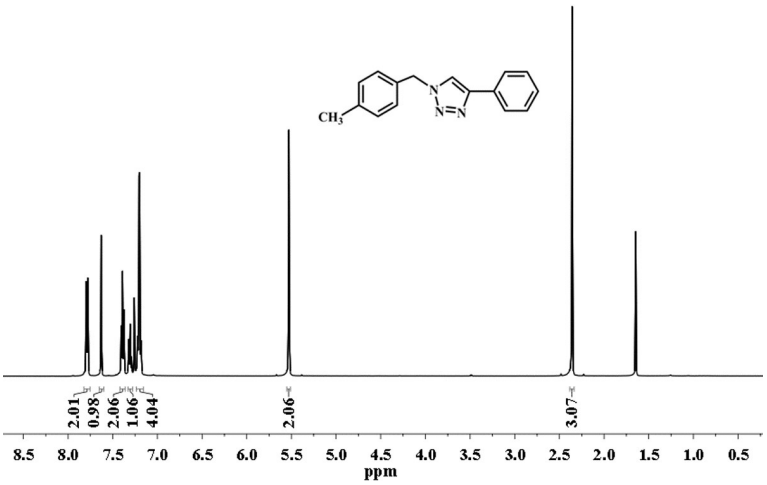

Fig. S10 ^{1}H NMR (500 MHz, $CDCl_3$) for 1-(4-methylbenzyl)-4-phenyl-1H-1,2,3-triazole.

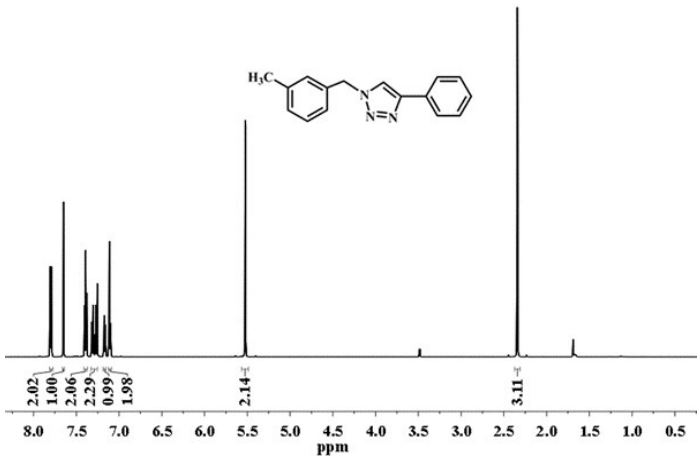

Fig. S11 ^{1}H NMR (500 MHz, $CDCl_3$) for 1-(3-methylbenzyl)-4-phenyl-1H-1,2,3-triazole.

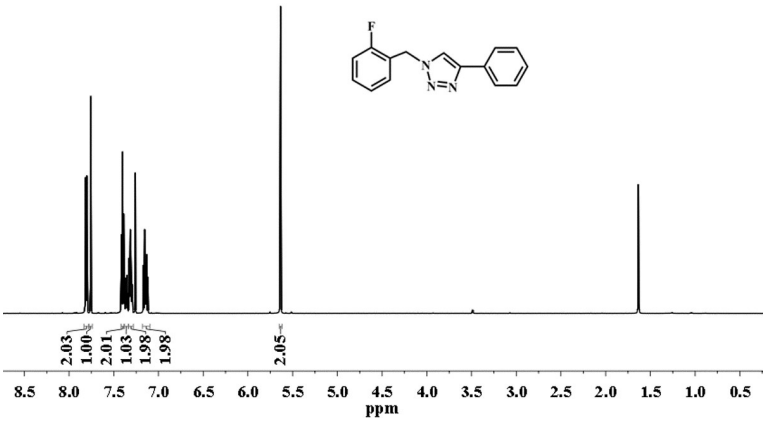

Fig. S12 ^{1}H NMR (500 MHz, $CDCl_3$) for 1-(2-fluorobenzyl)-4-phenyl-1H-1,2,3-triazole.

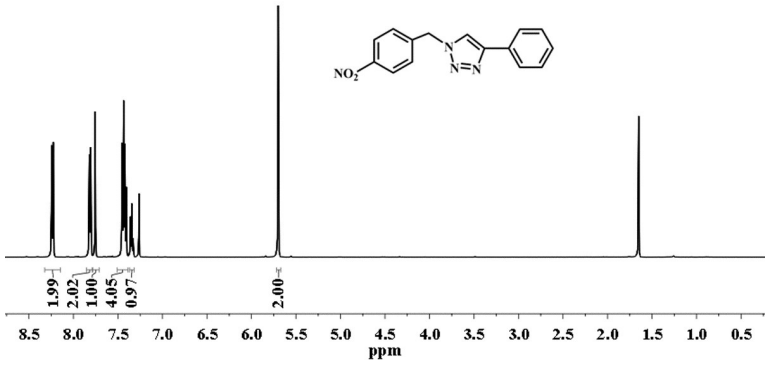

Fig. S13 ^{1}H NMR (500 MHz, $CDCl_3$) for 1-(4-nitrobenzyl)-4-phenyl-1H-1,2,3-triazole.

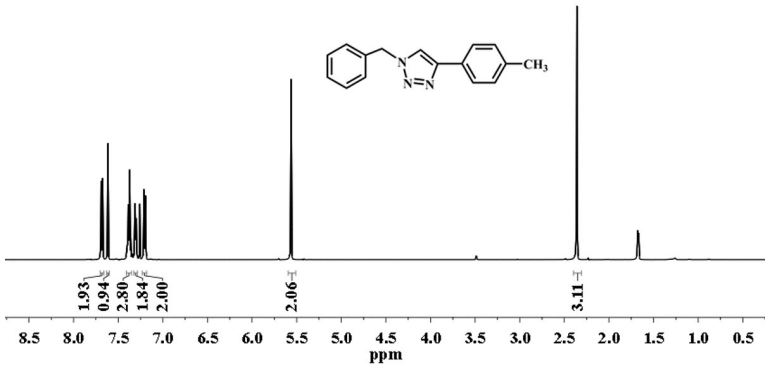

Fig. S14 ^{1}H NMR (500 MHz, $CDCl_3$) for 1-benzyl-4-(4-methoxyphenyl)-1H-1,2,3-triazole.

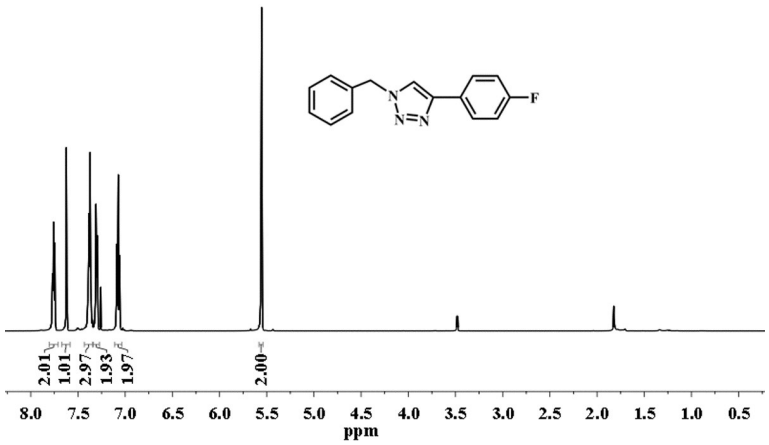

Fig. S15 ^{1}H NMR (500 MHz, $CDCl_3$) for 1-benzyl-4-(4-fluorophenyl)-1H-1,2,3-triazole.

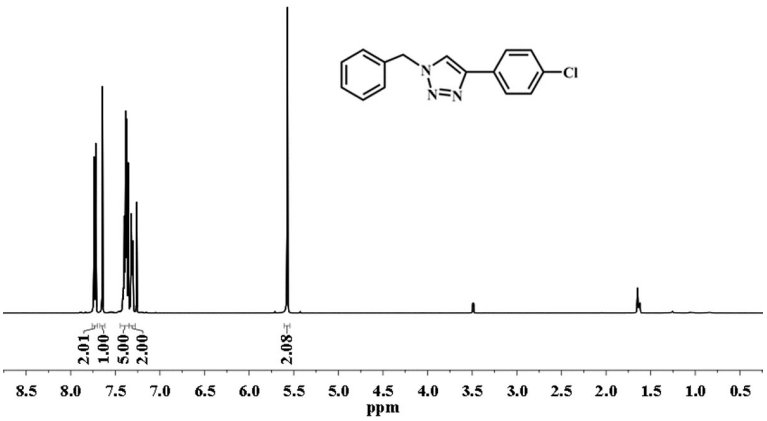

Fig. S16 ^{1}H NMR (500 MHz, $CDCl_3$) for 1-benzyl-4-(4-chlorophenyl)-1H-1,2,3-triazole.

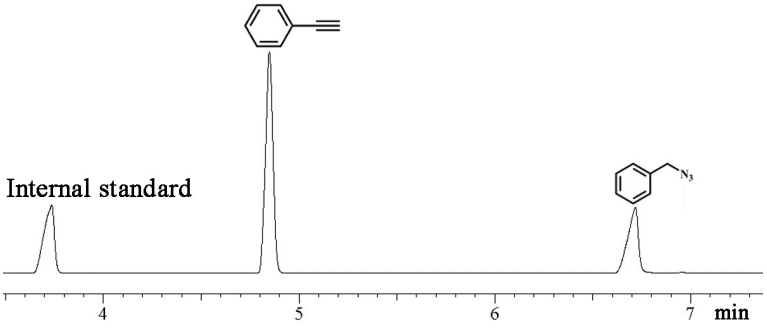

(a)

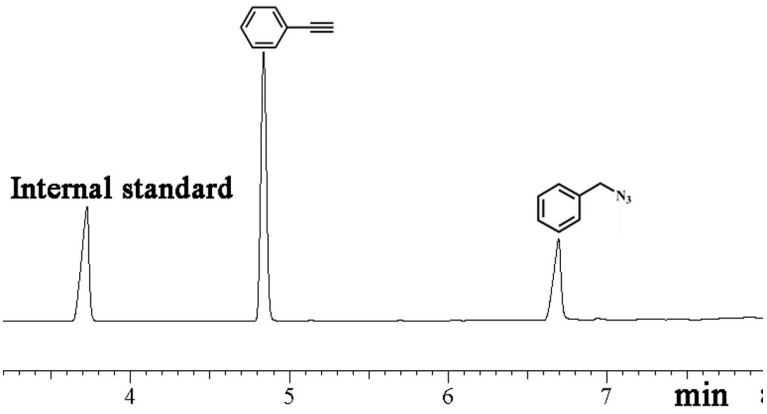

(b)

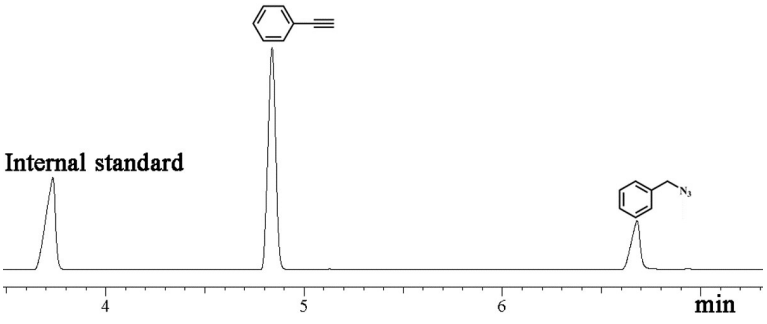

(c)

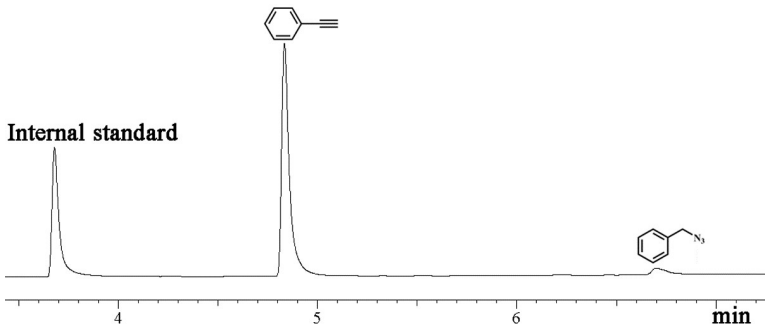
Internal standard
4
5
6
min

(d)

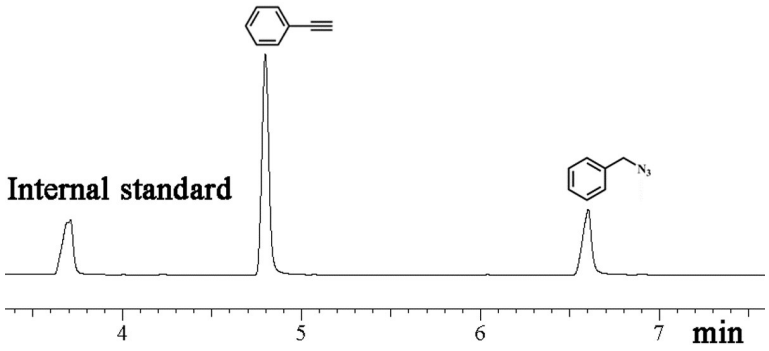
Internal standard
4
5
6
7
min

(e)

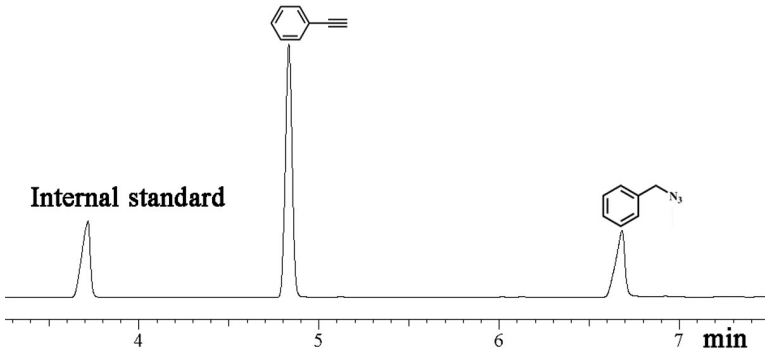
Internal standard
4
5
6
7
min

(f)

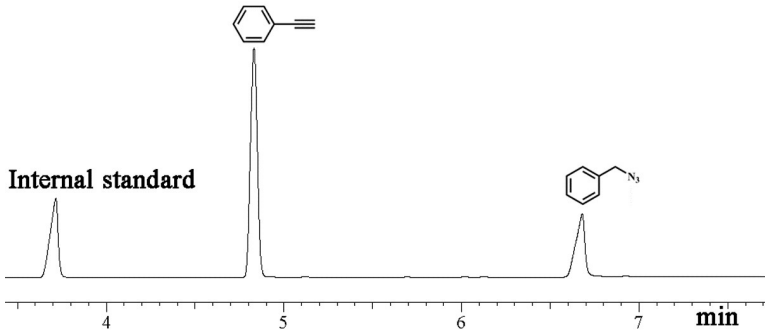
Internal standard
4
5
6
7
min

(g)

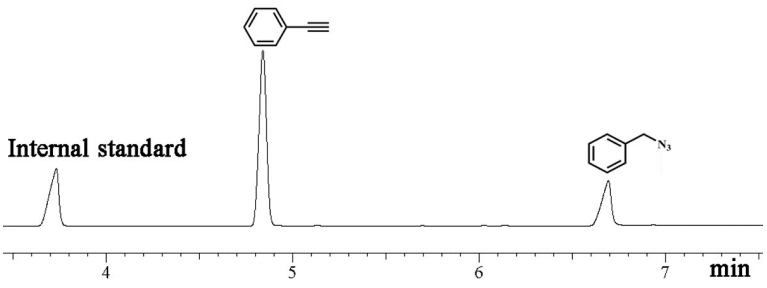

(h)

Fig. S17 GC of reactions of benzyl azide and phenylacetylene with kinetic and hot filtration experiments: (a) **1** (5 mg), MeOH, 1h, 80°C. (b) **1** (5 mg), MeOH, 2h, 80°C. (c) **1** (5 mg), MeOH, 3h, 80 °C. (d) **1** (5 mg), MeOH, 4h, 80°C. (e) MeOH, 2 h, the filtrate after removing **1** after 1 h of the reaction. (f) MeOH, 3 h, the filtrate after removing **1** after 1 h of the reaction. (g) MeOH, 4 h, the filtrate after removing **1** after 1 h of the reaction. (h) MeOH, 5 h, the filtrate after removing **1** after 1 h of the reaction.

(a)

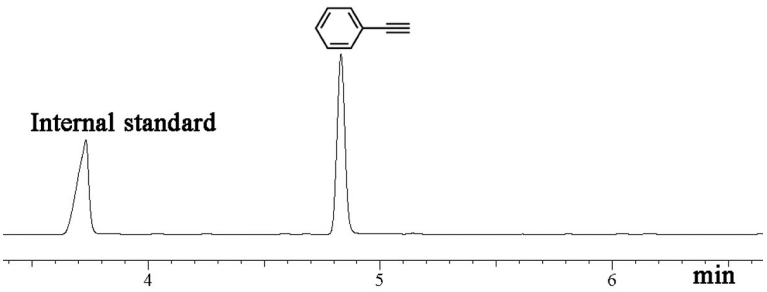

(b)

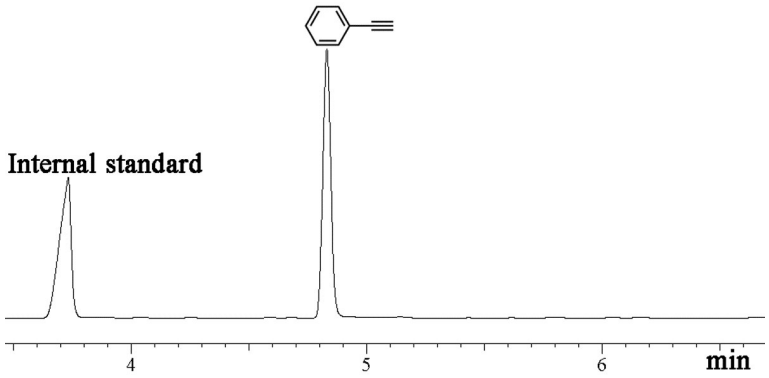

(c)

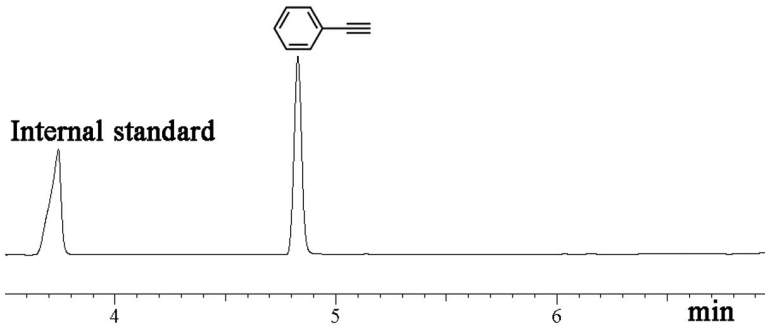

(d)

Fig. S18 GC of reactions between benzyl azide and phenylacetylene in different circles: (a) the first circle. (b) the second circle. (c) the third circle. (d) the fourth circle.

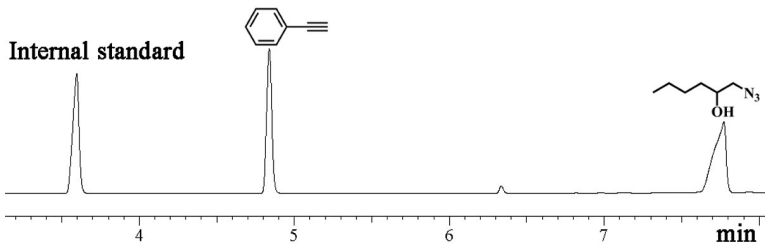

(a)

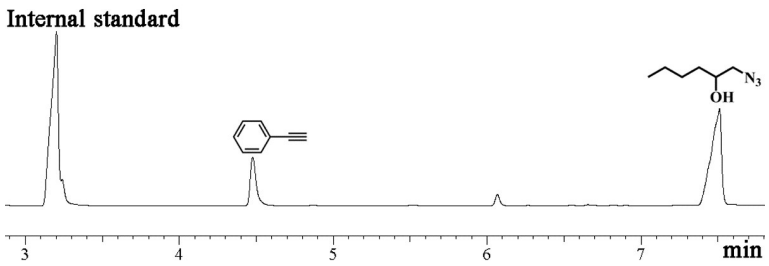

(b)

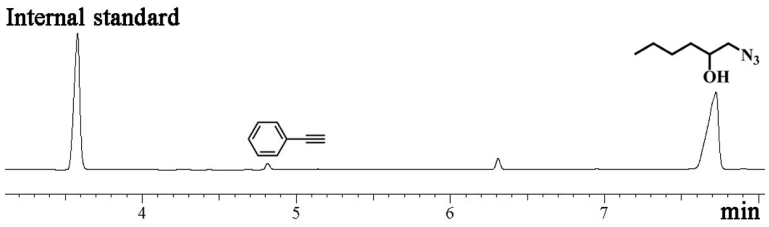
Internal standard
N3
OH
4
5
6
7
min

(c)

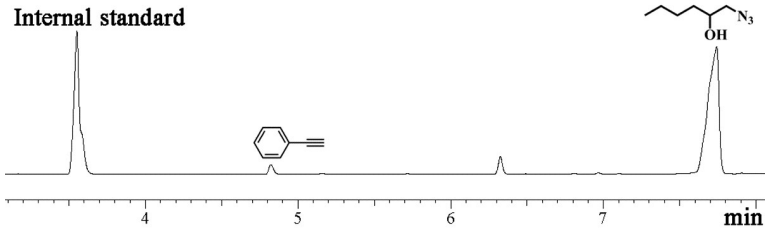
Internal standard
N3
OH
4
5
6
7
min

(d)

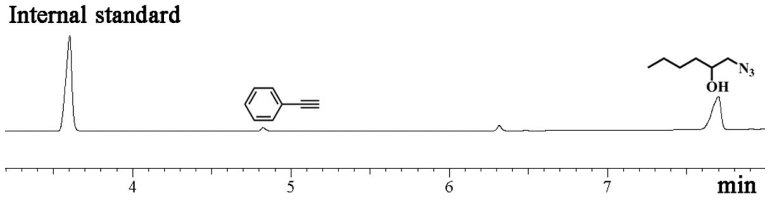
Internal standard
N3
OH
4
5
6
7
min

(e)

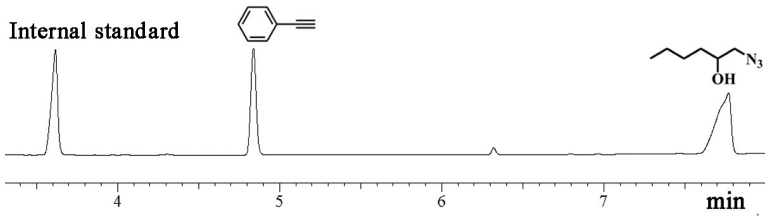
Internal standard
N3
OH
4
5
6
7
min

(f)

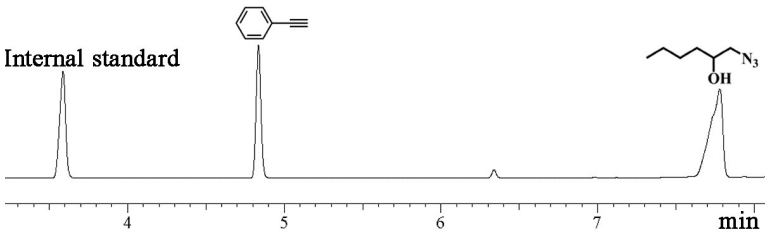
Internal standard
N3
OH
4
5
6
7
min

(g)

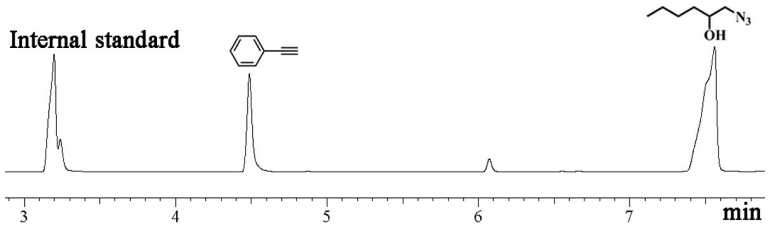
Internal standard
N3
OH
3
4
5
6
7
min

(h)

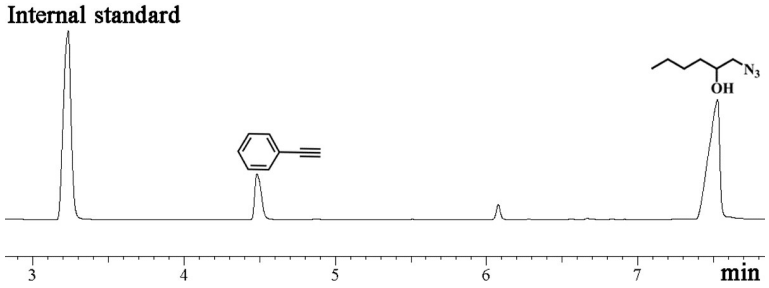

(i)

Fig. S19 GC of reactions of 1-azido-2-hexanol and phenylacetylene under different conditions: (a) **1** (0 mg), MeOH, 8 h, 80°C. (b) **1** (5 mg), MeOH, 8 h, 80 °C. (c) **1** (10 mg), MeOH, 8 h, 80 °C. (d) **1** (15 mg), MeOH, 8 h, 80°C. (e) **1** (10 mg), EtOH, 8 h, 80°C. (f) **1** (10 mg), MeCN, 8 h, 80°C. (g) **1** (10 mg), MeOH, 8 h, 25°C. (h) **1** (10 mg), MeOH, 8 h, 40°C. (i) **1** (10 mg), MeOH, 8 h, 60 °C.

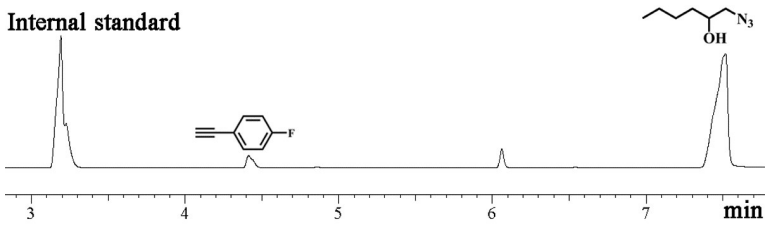

(a)

(b)

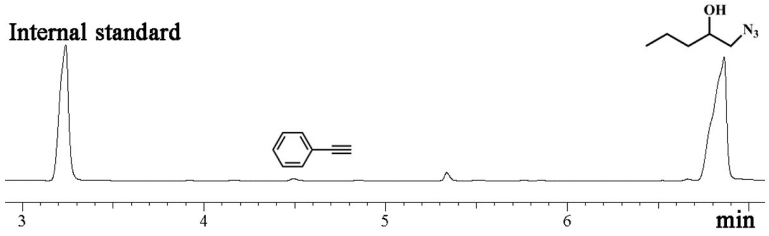

(c)

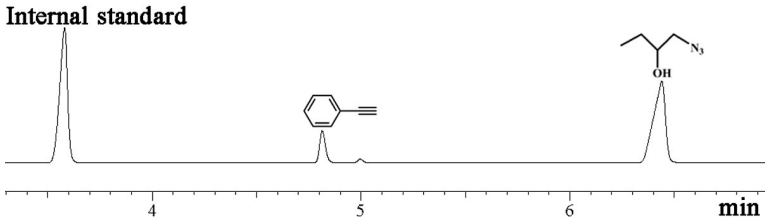

(d)

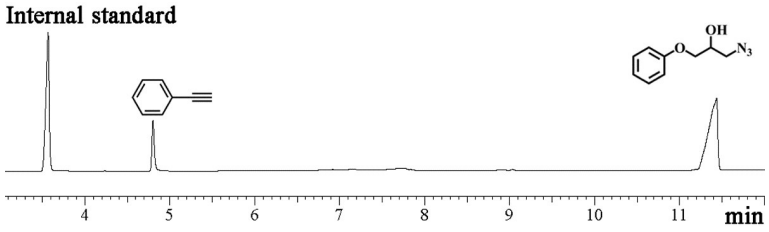

(e)

Fig. S20 GC of reactions of substituted β-OH azides and phenylacetylenes with different groups under the same condition (**1** (10 mg), MeOH, 8 h, 80 °C):

(a)1-azido-2-hexanol and phenylacetylene as substrates.

(b) 1-azido-2-hexanol and 1-ethynyl-4-fluorobenzene as substrates.

(c)1-azido-2-pentanol and phenylacetylene as substrates.

(d) 1-azido-2-butanol and phenylacetylene as substrates.

(e) 1-azido-3-phenoxy-2-propanol and phenylacetylene as substrates.

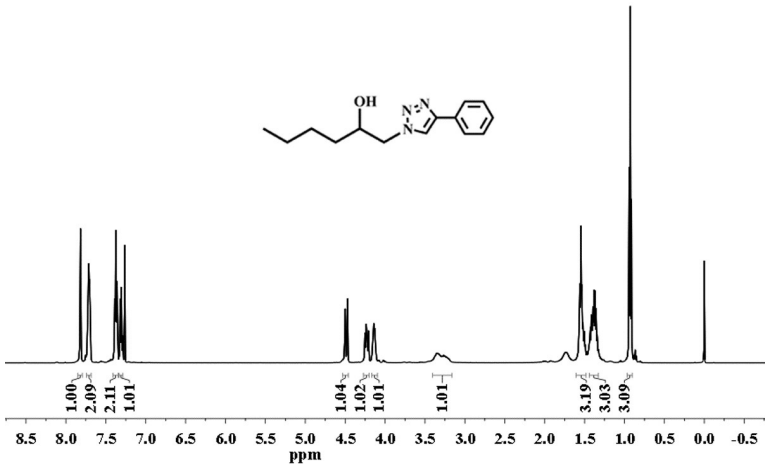

Fig. S21 ^{1}H NMR (500 MHz, $CDCl_3$) for 1-(4-phenyl-1H-1,2,3-triazol-1-yl)hexan-2-ol.

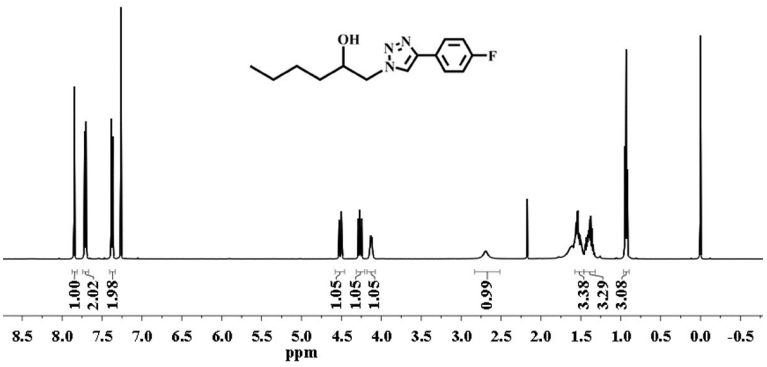

Fig. S22 ^{1}H NMR (500 MHz, $CDCl_3$) for 1-(4-(4-fluorophenyl)-1H-1,2,3-triazol-1-yl)hexan-2-ol.

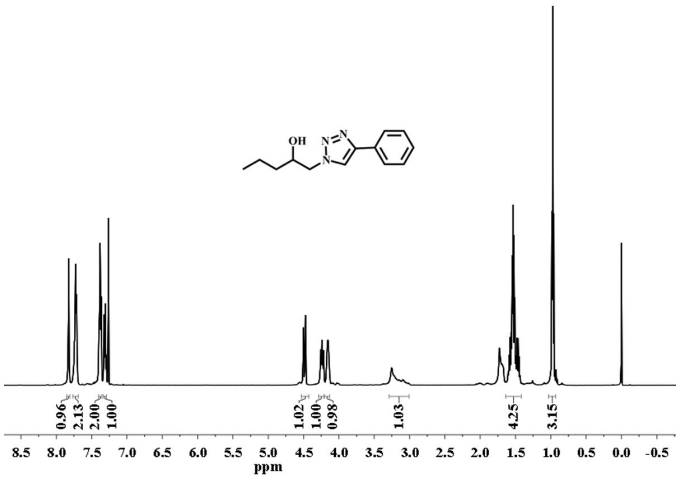

Fig. S23 ^{1}H NMR (500 MHz, $CDCl_3$) for 1-(4-phenyl-1H-1,2,3-triazol-1-yl)pentan-2-ol.

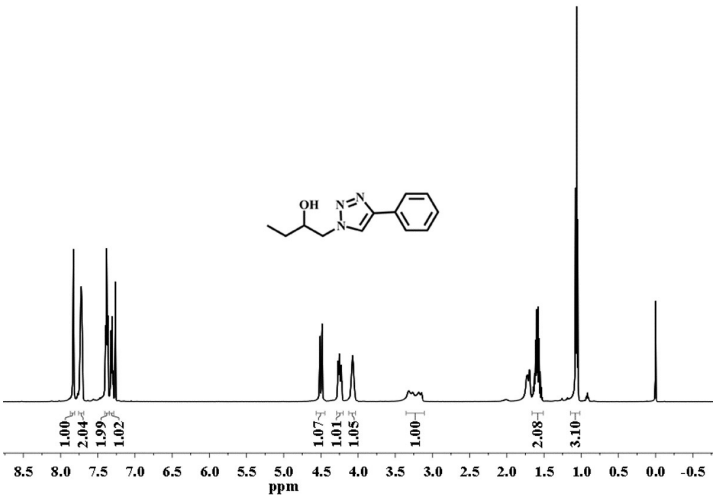

Fig. S24 ^{1}H NMR (500 MHz, $CDCl_3$) for 1-(4-phenyl-1H-1,2,3-triazol-1-yl)butan-2-ol.

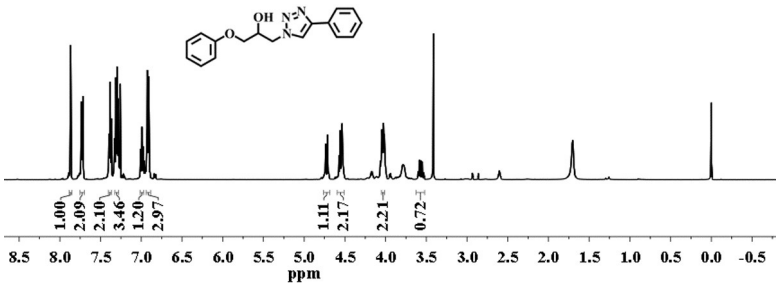

Fig. S25 ^{1}H NMR (500 MHz, $CDCl_3$) for 1-phenoxy-3-(4-phenyl-1H-1,2,3-triazol-1-yl) propan-2-ol.

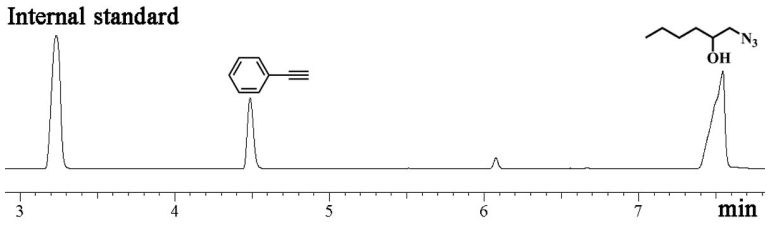

(a)

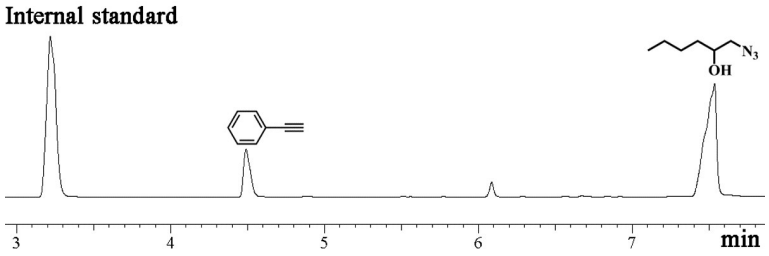

(b)

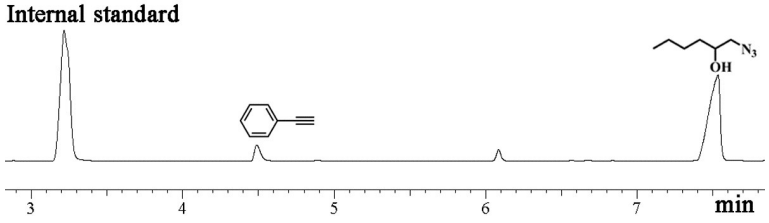

(c)

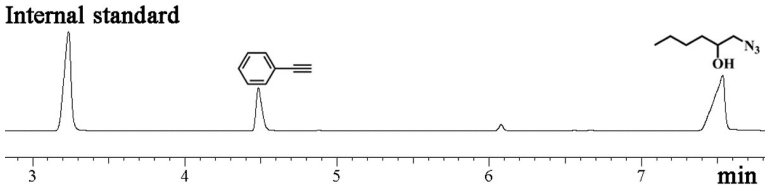

(d)

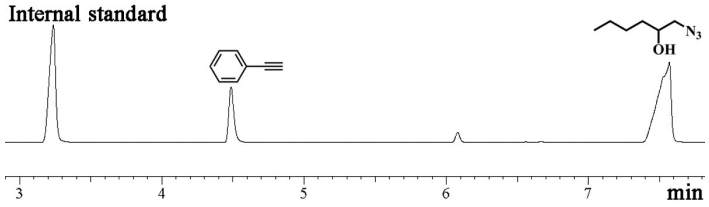

(e)

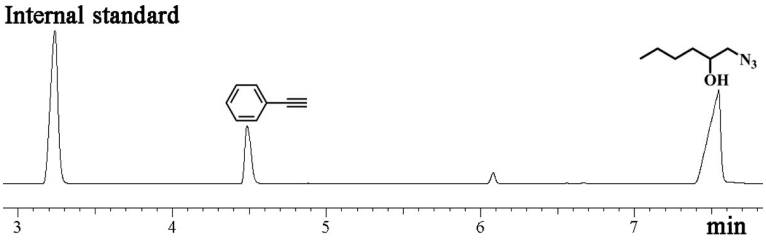

(f)

Fig. S26 GC of reactions of 1-azido-2-hexanol and phenylacetylene with kinetic and hot filtration experiments: (a) **1** (10 mg), MeOH, 2h, 80°C; (b) **1** (10 mg), MeOH, 4h, 80°C. (c) **1** (10 mg), MeOH, 6h, 80 °C. (d) MeOH, 4 h, the filtrate after removing **1** after 2 h of the reaction. (e) MeOH, 6 h, the filtrate after removing **1** after 2 h of the reaction. (f) MeOH, 8 h, the filtrate after removing **1** after 2 h of the reaction.

(a)

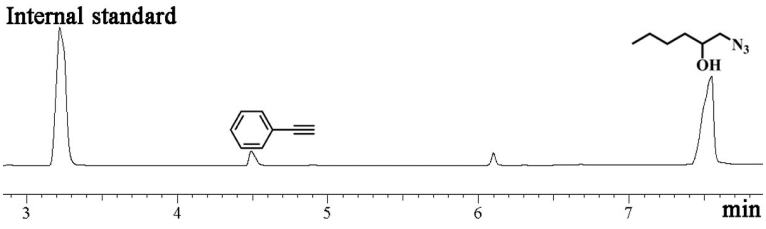

(b)

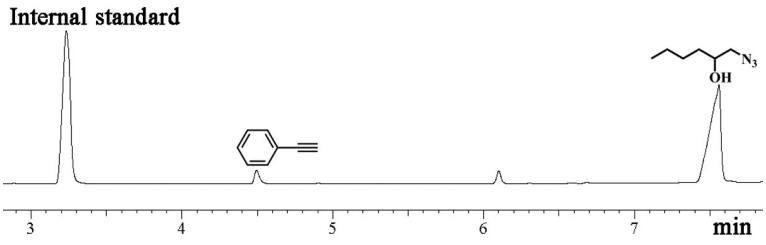

(c)

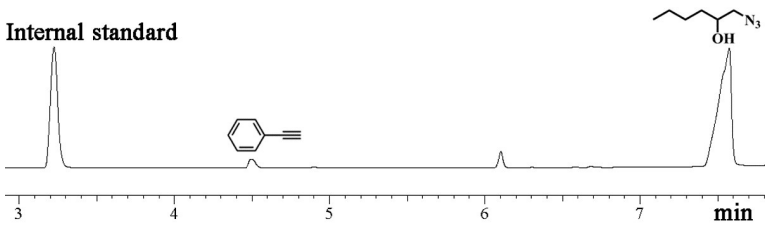

(d)

Fig. S27 GC of reactions of 1-azido-2-hexanol and phenylacetylene in different circles: (a) the first circle. (b) the second circle. (c) the third circle. (d) the fourth circle.